AUT Journal of Civil Engineering

AUT J. Civil Eng., 9(2) (2025) 111-128
DOI: 10.22060/ajce.2025.23851.5904

Prediction of the shear strength of SCS Panel with Box Profile shear connectors using numerical modeling and GEP algorithm

Seyed Hashem Khatibi, Hamed Ghohani Arab*, Mahmoud Miri

Department of Civil Engineering, University of Sistan and Baluchestan, Zahedan, Iran.

ABSTRACT: Steel-concrete-steel (SCS) sandwich structures consist of two steel faceplates and a concrete core, interconnected through mechanical shear connectors to form an integrated composite system. Among various shear connectors, box-profile (BP) shear connectors have demonstrated superior shear strength. Despite this, no equation has been developed to estimate the shear strength of BP shear connectors, unlike the well-established provisions for stud-bolt connectors. This study aims to address this gap by proposing a predictive equation for the shear strength of BP shear connectors using the Taguchi design of experiments (DOE). Key parameters, including the thickness, width, and yield strength of BP shear connectors, as well as the thickness and compressive strength of the concrete core, were systematically analyzed. A total of 32 specimens were designed, and their behavior was validated through experimental push-out tests and simulations, focusing on failure modes and load-slip curves. Finite element (FE) analysis and gene expression programming (GEP) were employed to develop a predictive equation incorporating two failure modes: concrete failure and BP failure. The proposed equation was rigorously evaluated against existing code provisions using statistical metrics such as root-mean-square error (RMSE), mean absolute percentage error (MAPE), and Nash-Sutcliffe efficiency (NSE). Results demonstrated the superior accuracy and reliability of the proposed model. This study provides a robust framework for designing BP shear connectors, addressing a critical gap in the design of SCS sandwich structures and advancing their practical application.

Review History:

Received: Jan. 21, 2025
Revised: May, 12, 2025
Accepted: Jun. 26, 2025
Available Online: Aug. 27, 2025

Keywords:

Steel-Concrete-Steel
BP Connectors
Shear Connectors
Push-out
SCS

1- Introduction

Steel-concrete-steel (SCS) sandwich structures consist of a concrete core covered by two thin steel faceplates. Epoxy adhesives were initially proposed to connect the components of an SCS structure. However, epoxy adhesives could not resist interlayer shear forces and were thus replaced with mechanical shear connectors. Researchers have proposed a variety of shear connectors, *e.g.*, angle shear connectors(Fig.1(a))[1, 2], stud-bolt connectors(Fig.1(b))[3-6], bi-steel connectors(Fig.1(c))[7-9], J-hook connectors(Fig.1(d))[10-12], separately corrugated strip (Fig.1(e))[13-16] and box-profile (BP) connectors(Fig.1(f))[17-19], each with a remarkably different shape and behavior. In recent decades, this system has massively grown in the civil engineering literature. It has been used in the construction of immersed tubes (tunnels)[20], bridges[21], offshore decks[22], oil reservoirs, and shear walls[23]. Earlier numerical and analytical studies on SCS sandwich structures are reviewed below.

Anandavalli *et al.* (2013) analyzed SCS beams with bi-steel shear connectors numerically. An SCS beam with bi-steel shear connectors was numerically modeled and validated first in their study. Some specimens were then designed and simulated to investigate the effects of the steel faceplate thickness, bi-steel shear connector diameter, and bi-steel shear connector orientation. The system was optimized at a shear connector orientation of 40–50 degrees, a steel faceplate thickness of 10 mm, and a shear connector diameter of 12 mm[8].

Chang-Hui Li *et al.* (2021) modeled and validated push-out tests of modified angle shear connectors. A total of 51 specimens were then modelled to analyse the effects of the bolt diameter, bolt hole distance, angle size, and concrete core strength on load-slip behavior. They proposed an equation to predict the load-slip behavior of the modified angle shear connector[24].

Yousefi *et al.* (2023) studied the flexural behavior of SCS sandwich slabs with stud-bolt shear connectors numerically under quasi-static concentrated loads. Experimental specimens were then modeled and validated using the finite element (FE) analysis. They also investigated the effects of the steel faceplate thickness, stud-bolt thickness, core thickness, and the centre-to-centre distance of the stud-bolts on the failure modes and load-displacement curve. They then employed a complete factorial design of experiment (DOE) to design numerical models to predict the ultimate strength of the slabs. Finally, a simple equation sandwich slabs with

*Corresponding author's email: ghohani@eng.usb.ac.ir

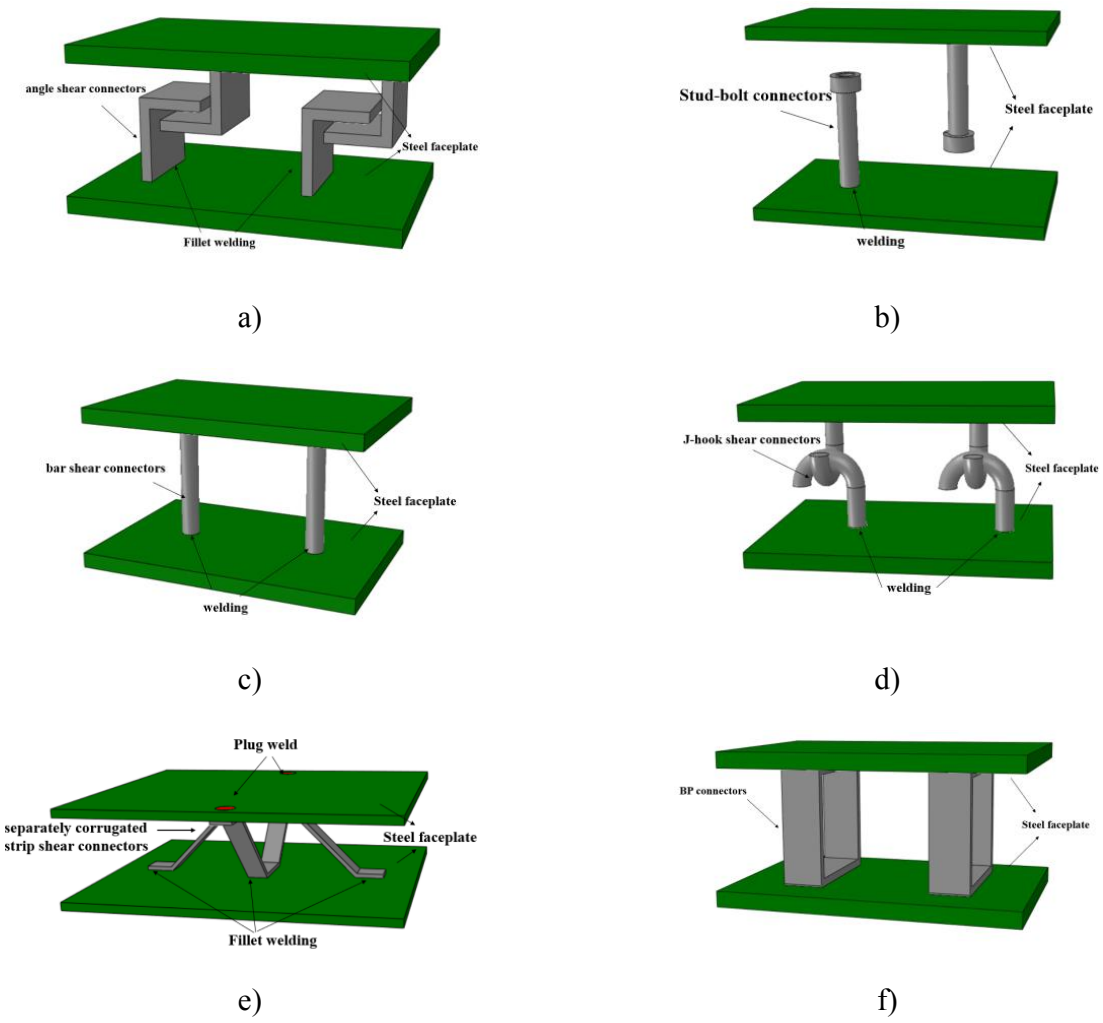

Fig. 1. Shear connectors in SCS sandwiches, angle shear connectors(a), Double skin concrete system with stud shear connectors(b), bar shear connectors in Bi-steel system(c), J-hook shear connectors(d), separately corrugated strip shear connectors(SCSC)(e), Box Profile Shear connectors(f).

stud-bolt shear connectors[25].

Every proposed shear connector type has certain advantages and disadvantages. For example, headed shear connectors lack an integrated connection to the steel faceplates, and the steel faceplates are detached once cracking occurs under impact. Despite their high detachment resistance, headed shear connectors require friction welding, have thickness limitations, and are expensive. As a result, J-hook shear connectors were proposed to handle such thickness limitations. However, the interlocking of all hooks in J-hook systems is difficult on a large scale.

Therefore, Khatibi *et al.* (2022) proposed box-profile (BP) shear connectors. These shear connectors have no thickness limitations and integrate the two shear faceplates. As a result, BP shear connectors do not experience a sharp reduction in detachment resistance upon concrete core cracking with stud-bolt shear connectors. Moreover, BP shear connectors do not require bending, as they are rolled box profiles, unlike discrete strip connectors and J-hook shear connectors. They have simple fabrication and show more excellent detachment resistance in light of their larger welded area[18].

Fig. 2 depicts the fabrication phases of a single BP shear connector. The BP connector is filled-welded on one end to the steel faceplate (Fig. 2(a)). The other steel faceplate is placed, and a slot weld is implemented (Fig. 2(b)). Finally, molding and concreting are performed (Fig. 2(c)).

Khatibi *et al.* (2022) conducted push-out tests on BP shear connectors to evaluate their interlayer shear strength[19]. Eight SCS sandwich structures with BP connectors were subjected to push-out tests to investigate the effects of geometric parameters, *e.g.*, the concrete thickness, BP thickness and width, and BP configuration, on the interlayer shear strength. Furthermore, no reliable equation was proposed to predict shear strength due to the limited number of specimens.

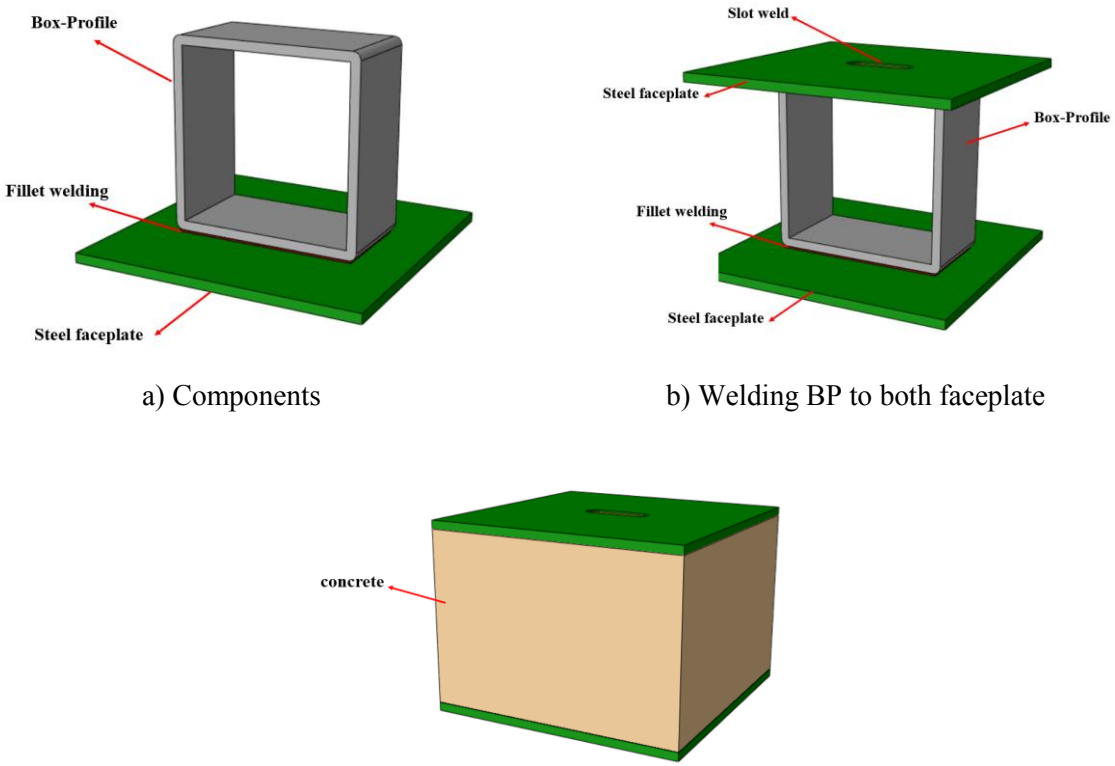

a) Components

b) Welding BP to both faceplate

c) Concrete casting

Fig. 2. SCS construction steps with BP shear connector

Khatibi *et al.* (2023) investigated SCS moment beams with BP shear connectors experimentally and numerically[18]. They conducted three-point flexural tests on nine beam specimens to evaluate the effects of the BP connector thickness and width, and concrete core thickness. They also studied the effects of concrete core strength and the BP connector orientation on the flexural behavior of the SCS beams through the FE analysis. Despite these advancements, there remains a significant gap in understanding the shear behavior of double-welded BP shear connectors, as shear failure is one of the critical modes of failure in SCS beams. Understanding the shear capacity of SCS beams is of great importance; however, due to the limited number of laboratory samples, it has not been possible to develop a relationship for estimating the shear resistance of double-welded BP shear connectors.

The novelty and primary contribution of this study lie in addressing this critical research gap concerning the estimation of shear resistance for BP shear connectors. While previous research has explored various types of shear connectors, including discrete strip shear connectors, stud connectors, channel connectors, and hook-type connectors, comprehensive studies on the behavior and prediction of shear resistance for hollow section shear connectors have yet to be conducted. This study aims to fill this void by examining the simultaneous effects of geometric parameters, concrete core strength, and shear connectors on interlaminar shear resistance in SCS structures.

The key contribution of this research is to provide a relationship for the shear resistance of double-welded BP shear connectors. The push-out specimens in Khatibi *et al.*'s study (2022) were fabricated and tested, as shown in Table 1. They were simulated using the finite element method (FEM) in ABAQUS and validated in terms of the failure mode and load-slip curve.

Various factors, such as the strength of the concrete core, the thickness and width of the shear connectors, and the thickness of the concrete core, can influence the shear resistance and behavior of SCS samples. The simultaneous examination of the effects of these factors is quite complex and debatable. Therefore, to develop a relationship for estimating shear resistance, it is essential to analyze the combined effects of the variables. This requires numerous modeling efforts, which can be time-consuming and costly.

The Taguchi experimental design method is an effective technique widely utilized in engineering analysis. This method is a type of experimental design that employs orthogonal arrays to reduce the number of experiments while minimizing the effects of uncontrollable variables. One of the greatest advantages of this approach is the reduction in

Table 1. The geometric dimensions of the BPC sandwich system [28].

Specimen	b_c (mm)	t_c (mm)	h_{con} (mm)
N-1	20	4	100
N-2	30	4	100
N-3	40	4	100
N-4	20	5	100
N-5	20	6	100
N-6	20	4	120
N-7	20	4	130

***Notes:** Width of steel face plates b = 260 mm; Concrete thickness h_{con}= Connector height h_c

testing time, which helps optimize costs and facilitates the identification of influential factors within a short timeframe. In this method, the main parameters affecting the results of a process are organized in different rows of an orthogonal array.

The Taguchi method was then adopted to design and simulate 32 models to reflect the interrelationships of geometric parameters, concrete core strength, and steel faceplate strength. Finally, GEP was used to develop an equation based on the failure modes of the concrete core and BP connectors. The equation was evaluated using the root-mean-square error (RMSE), mean absolute percentage error (MAPE), and Nash-Sutcliffe efficiency (NSE). Moreover, b_c, t_c, and h_{con} denote the BP width, BP thickness, and concrete core thickness, respectively (Table 1, Fig.3).

The Push-out test has been utilized as a standard method to evaluate the shear behavior of BP connectors. Given its strong capability in modeling shear resistance and interlayer slip, it has also been applied to assess the shear behavior of CSC, J-hook, and stud bolt shear connectors[15, 26, 27]. However, under vertical loading conditions (orthogonal to the Push-out test), the force transfer mechanism between the concrete core and steel plates differs, which may influence stress concentration in the weld zone and confined concrete behavior. Fig4 . illustrates the Push-out test setup.

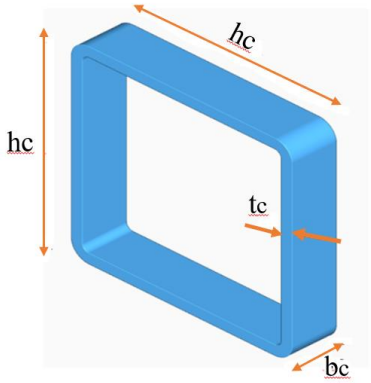

Fig. 3. The geometric specifications of the BP shear connector.

2- FE Model

The experimental specimens were numerically simulated using explicit dynamic analysis in ABAQUS.

2- 1- Steel Faceplate Modelling

The isotropic strain-hardening rule and elastoplastic constitutive model with the von Mises yield criterion were employed to model the steel faceplates. Bilinear behavior was defined for the faceplates (Table 2).

2- 2- Concrete Core Modelling

The plastic-damage model in the ABAQUS library was used to simulate the concrete core[28] .Compressive stress-strain equations were employed to predict the compressive behavior of the concrete core[25]:

$$\sigma_c = \frac{n f_c \varepsilon_c}{\varepsilon_0 \left(n - 1 + \left(\frac{\varepsilon_c}{\varepsilon_0} \right)^{nk} \right)} \quad (1)$$

$$n = 0.8 + \frac{f_c}{17} \quad (2)$$

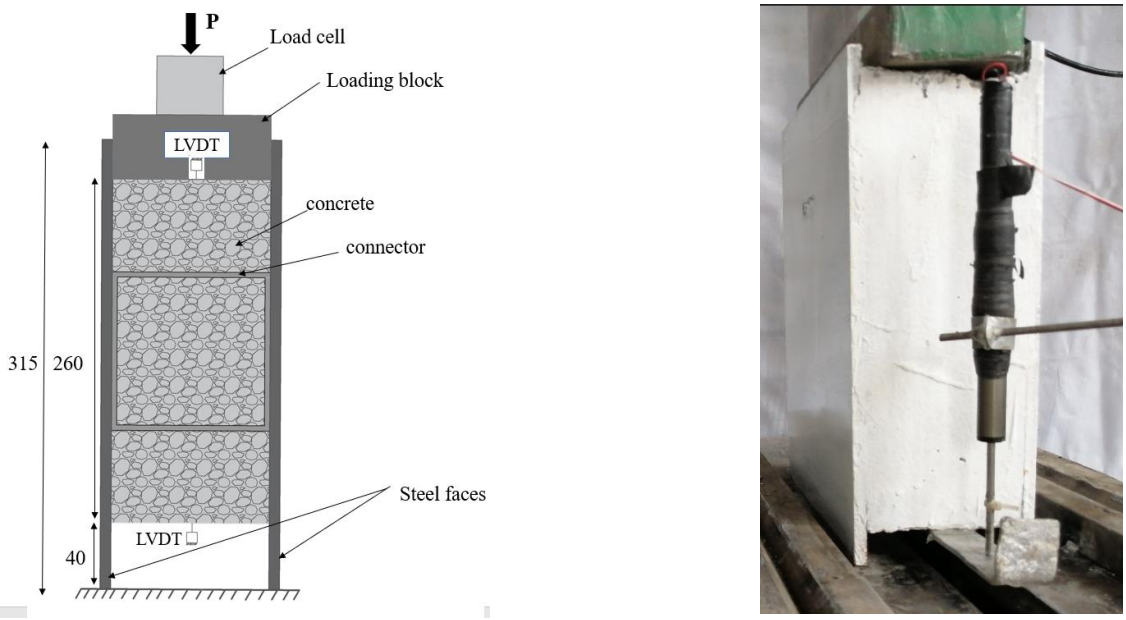

Fig. 4. Push-out test setup[19].

Table 2. Mechanical properties of steel faceplates and BP connectors derived from direct tensile test.

specimen	Yield stress (Mpa)	Ultimate stress (Mpa)	Strain in ultimate stress	E_s (Gpa)
Profile 100×100×4	260	387.9	0.33	204
Profile 100×100×5	390	533.7	0.26	206
Profile 100×100×6	385	509	0.26	209
Profile 120×120×4	295	411.6	0.27	202
Profile 130×130×4	285	433.2	0.3	204
Plate (8mm)	275	485	0.26	205

$$\begin{cases} k = 0.67 + \left(\frac{f_c}{62}\right) & \varepsilon_c > \varepsilon_0 \\ k = 1 & \varepsilon_c \le \varepsilon_0 \end{cases} \quad (3)$$

where f_c is the compressive strength of a cylindrical concrete specimen, ε_0 is the strain corresponding to f_c, ε_c is the compressive stress, and ε_c is the compressive strain.

Fig. 5 plots the compressive stress-strain curve of concrete with a compressive strength of 39.5 MPa obtained from Eq. (1). This curve was used to simulate the concrete cores of the SCS sandwich beams.

For the specimens examined in this study, the absence of confining plates has resulted in concrete behavior being predominantly influenced by slippage. Therefore, equations related to confined concrete were not utilized in this model. However, for other conditions, such as SCS beams in flexural tests, more precise modeling that accounts for confinement effects will be necessary.

Huang *et al.* (2015) defined the damage parameter as Eq. (4) and (5)[3]:

$$0 \le d_c = 1 - \frac{\sigma_c + n_c f_c}{E_c\left(\frac{n_c f_c}{E_c} + \varepsilon_c\right)} \le 1 \quad (4)$$

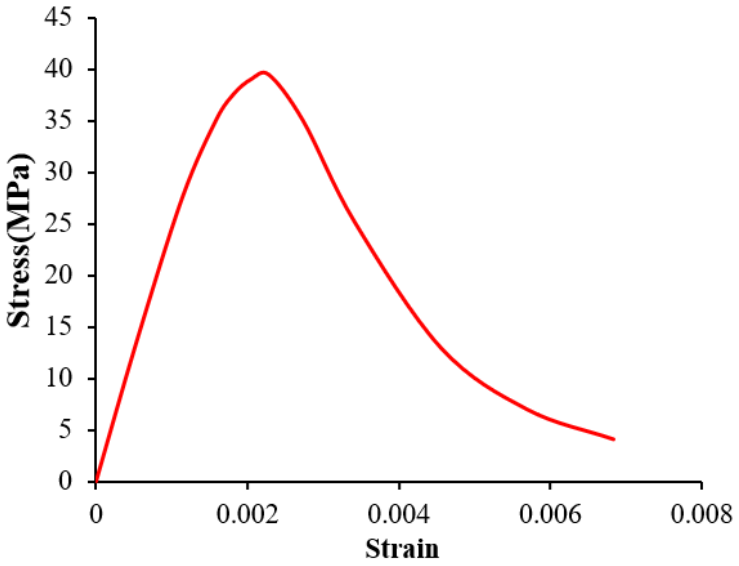

Fig. 5. Stress-strain curve of regular concrete.

$$0 \le d_t = 1 - \frac{\sigma_t + n_t f_t}{E_c\left(\frac{n_t f_t}{E_c} + \varepsilon_t\right)} \le 1 \quad (5)$$

where d_c and d_t denote compressive damage and tensile damage, while n_c and n_t are the compressive and tensile factors (ranging from 0 to 1), respectively. Furthermore, f_t and E_c refer to the tensile strength and the elasticity modulus of concrete, respectively. The concrete was assumed to show linear behavior below the tensile strength, which was set to 3.1 MPa[19]. Moreover, the dilation angle ψ, plastic potential surface eccentricity, the failure function indices (*i.e.*, biaxial-uniaxial compressive stress ratio) $f = f_{b0}/f_{c0}$ ‘, stress plane deviation parameter or confinement angle *k*, and viscoplastic parameter were set to 30◦, 0.1, 1.16, 0.667, and 0.001, respectively.

3- Boundary Conditions and Loading

The supports were constrained in three directions in the push-out test (Fig. 6), and a quasi-static load was applied to a rigid component. Surface-to-surface contact was assumed between the concrete core and steel faceplates and between the concrete core and BP shear connectors, with the hard contact formulation in the normal direction and the penalty friction in the tangential direction. A friction coefficient of 0.15 was assumed for the BP-core and faceplate-core interfaces.

Due to the complexity of the geometric model of the BP connector in the concrete core, explicit dynamic analysis and mass scaling were used to reduce the computational time in the quasi-static evaluation. The model mass was totally or partially increased virtually, and the stable time step

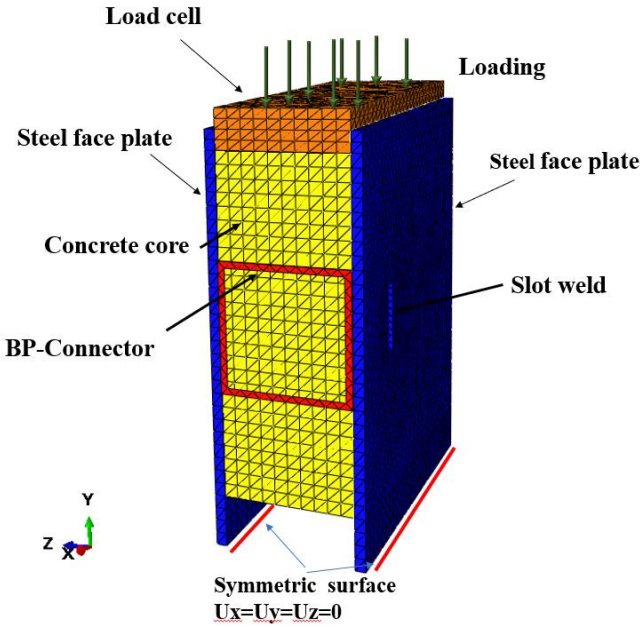

Fig. 6. FE model of the push-out test.

increased accordingly. Optimal mass scaling can shorten the computational time and maintain simulation accuracy within an acceptable range.

The loading time was set long enough to reduce the acceleration to nearly zero. An increase in the loading time would exponentially increase the computational time. Therefore, mass scaling was utilised for a given time step to minimise the computational time. The loading time and

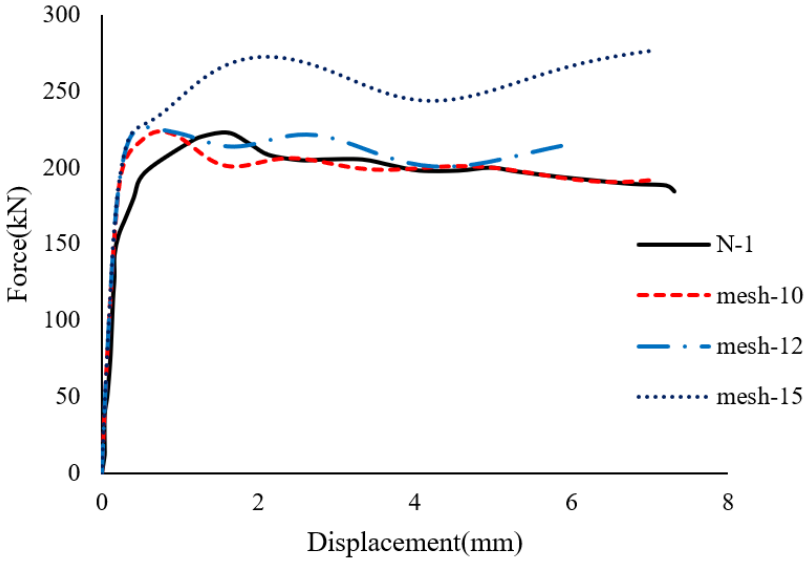

Fig. 7. Mesh size analysis for modelling.

Table 3. Experimental [19] vs. numerical ultimate strengths.

Specimen	F_{ut} (kN)	F_{un} (kN)	$\frac{F_{un}}{F_{ut}}$
N-1	222.82	223.43	0.997
N-2	306.5	300.4	1.02
N-3	393.85	384.57	1.024
N-4	268.48	266.7	1.007
N-5	297.87	293.15	1.016
N-6	236	225.5	1.047
N-7	257	258.58	0.994
Average			1.015
C.O.V			0.0002

*F_{ut} is the experimental ultimate strength, while F_{un} is the numerical ultimate strength

the time step should be assumed in a way that the model undergoes a quasi-static load.

4- Elements and Numerical Simulation

As viewed in Fig. 6, the experimental specimens include a load cell, steel faceplates, a concrete core, and BP shear connectors embedded in the concrete. Three-dimensional four-node continuous elements (C3D4) were used to simulate the SCS sandwich beams. Specimen N-1 was modeled using three mesh sizes of 10 mm, 12 mm, and 15 mm (Fig. 7). Based on the convergence of the simulations, a mesh size of 10 mm was found optimal. Moreover, a mesh size of 2.5 mm was applied to the slot welds on the steel faceplate to enhance the model accuracy.

5- Validation

Since mass scaling was used in the explicit dynamic analysis to model quasi-static loading, the external-to-internal energy ratio was controlled to remain below 10% in the specimens. The numerical and experimental load-displacement curves and failure modes were then compared.

5- 1- Validation of Load-Displacement Curves and Failure Modes

Fig. 8 compares the numerical and experimental load-displacement curves. Accordingly, the numerical model effectively predicted the load-displacement behavior of SCS sandwich specimens with BP shear connectors. Furthermore, the slight difference between the experimental and numerical data can be attributed to the bilinear modeling of the steel faceplates in the FE analysis. Table 3 compares the FE outputs and the experimental results in the ultimate strengths. According to Table 3, the mean and variance coefficient of the ultimate strength were reported as 1.015 and 0.0002, respectively. Therefore, the experimental and numerical ultimate strengths were acceptably consistent. Fig.9 indicates

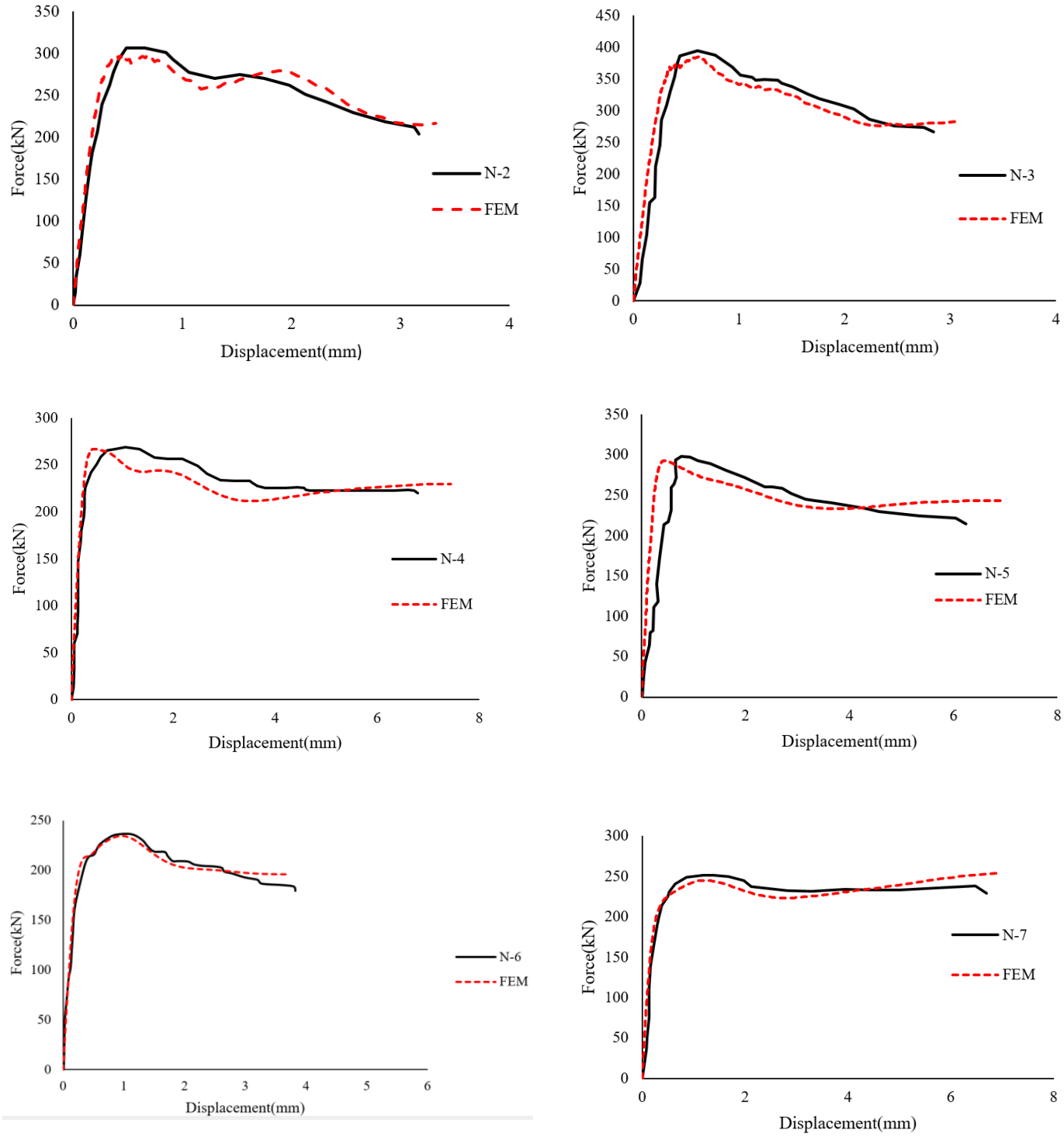

Fig. 8. Experimental [19] vs. numerical load-slip curves.

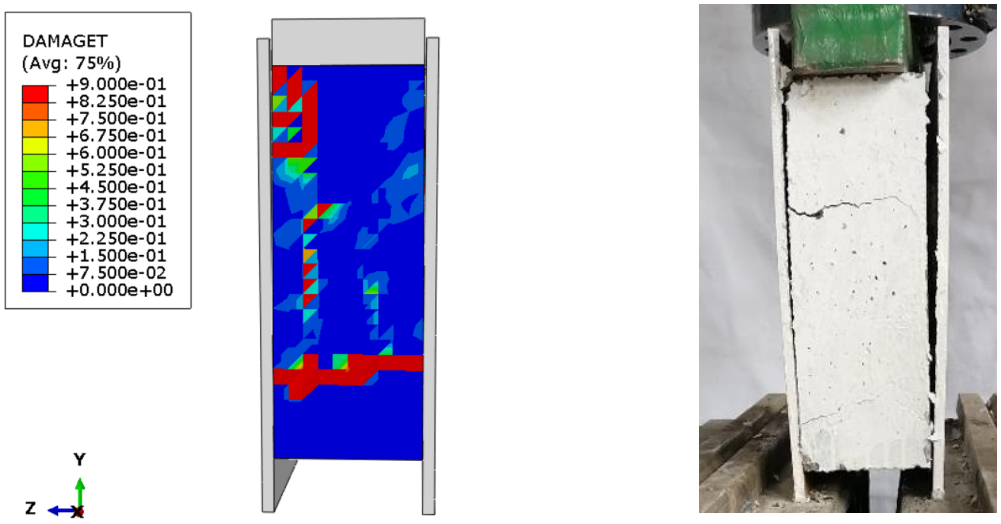

(a)Failure of Specimen N-1.

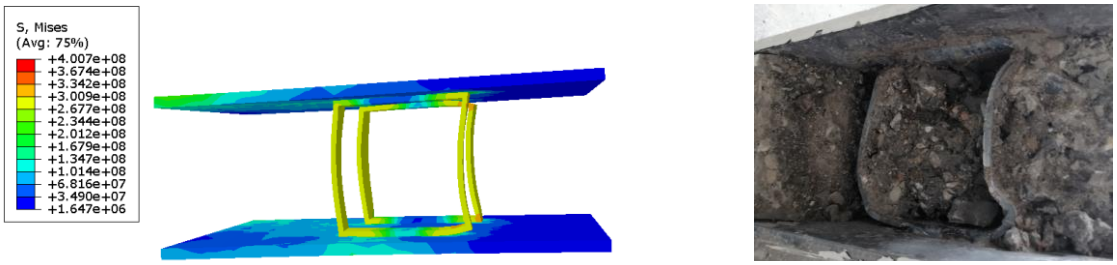

(b)BP connector deformation in Specimen N-2.

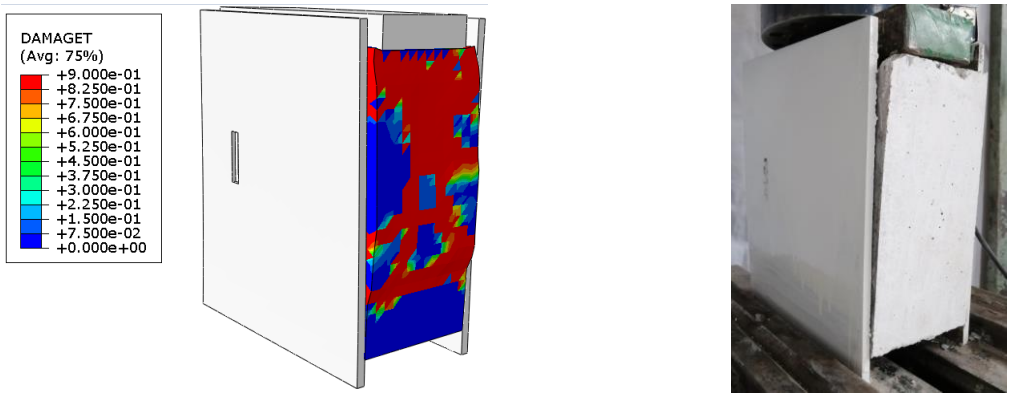

(a) Failure of Specimen N-6

Fig. 9. Experimental [19] vs. numerical failure modes.

that the numerical model effectively predicted the deformation mode of the BP shear connectors and the failure modes of the SCS specimens.

6- DOE

The Taguchi method was adopted to evaluate the effects of the interactions among geometric parameters, steel faceplate strength, and concrete core strength on the shear strength of BP connectors. A Taguchi design can be used to optimize the values of effective parameters in experiments. This approach utilizes statistical and engineering concepts and improves the quality of products. Since trial and error can be time-consuming and costly, design goals should be achieved through the minimum number of experiments. The Taguchi method consciously changes the input parameters to measure the change in the output. Therefore, the controllable input parameters can be systematically changed, evaluating their effects on the output parameters[29].

Five input parameters (*i.e.*, BP width (b_c), BP thickness (t_c), BP height (h_c), steel faceplate ultimate strength (F_u), and concrete core compressive strength (f_c)) were taken into account to consider the mutual effects (Table 4). The Taguchi method was then employed to model 32 DEOs. Table 5 reports the ultimate strengths and failure modes of the specimens.

In this study, two primary failure mechanisms in box connectors (BP) have been investigated:

Concrete core failure (CC), including slip, cracking, and crushing of concrete, which results from applied stresses and excessive deformation of the core. Shear connector failure (SC), comprising shear connector breakage or weld failure at the points where shear force is transferred between steel plates and the connector

7- GEP Model to Estimate Interlayer Shear Strength

Ferreira (2001) proposed GEP by integrating the gene programming (GP) approach and genetic algorithm (GA) with linear chromosomes of a fixed length and a structure similar to the decomposition trees in GP[35]. GEP generates a mathematical function using a given dataset [30]. In general, GEP is a GA-based approach that uses a population of data and selects data samples based on a competence function. Genetic changes are also applied using one or more operators (genes). The Roulette wheel selection method is used in GEP, and several genetic operators are simultaneously applied for proliferation, unlike in GP and GA. Proliferation is employed to maintain effective samples of the current population in the next generation. The mutation operator implements an internal random optimization of certain chromosomes[31]. Fig. 10 illustrates the flowchart of the GEP algorithm.

As shown in Table 6, concrete core failure and BP failure were dominant in the numerical analysis and experimental tests. Therefore, two GEP equations were developed based on BP strength and concrete core strengths.

Twenty-four of the numerical specimens (75%) were used as the training dataset, whereas eight numerical specimens (25%) were employed as the testing dataset. Table 5 presents the GEP parameters. RMSE minimization was selected as the competence criterion.

The GEP outputs were exploited to develop equations to estimate the shear strength of BP connectors based on the concrete core and BP failure modes. Concrete strength was used in the concrete failure equation, whereas the ultimate strength of the BP connectors was utilized in the BP failure equation.

The RMSE was minimised for Eq. (6):

$$p_u = \min\left\{\begin{array}{c}\sqrt{\sqrt{f_c}\times b_c}\times\dfrac{h_c\times t_c}{46.21}\\ \sqrt{\sqrt{f_u\times h_c}\times t_c\times b_c}\times\sqrt[3]{\text{Arctan}\left(\dfrac{t_c}{f_u}\right)\times h_c}\end{array}\right\} \quad (6)$$

Where h_{con} is the concrete core thickness, as both ends of BP shear connectors are welded, the concrete core thickness

Table 4. Input parameters and their levels in the Taguchi method.

parameters		LEVELS			
		Level 1	Level 2	Level 3	Level 4
BP width	b_c(mm)	10	20	30	40
BP thickness	t_c(mm)	4	6	8	10
BP height	h_c (mm)	100	120	140	160
steel faceplate ultimate strength	F_u(MPa)	370	520	-	-
concrete core compressive strength	f_c(MPa)	30	40	50	60

Table 5. Geometric parameters and the shear strength of the BP connectors.

Specimen	b_c(mm)	t_c(mm)	h_c (mm)	F_u(MPa)	f_c(MPa)	Failure Mode	F_{uN} by FEA (kN)
test-1	10	4	100	370	30	SC	76.85
test-2	20	6	100	370	40	CC	125.8
test-3	30	8	100	370	50	CC	266.95
test-4	40	10	100	370	60	CC	337.16
test-5	10	4	120	370	40	SC	80.12
test-6	20	6	120	370	30	CC	201.5
test-7	30	8	120	370	60	CC	302
test-8	40	10	120	370	50	CC	412.7
test-9	20	4	140	370	50	SC	141.1
test-10	10	6	140	370	60	SC	128.55
test-11	40	8	140	370	30	CC	305.45
test-12	30	10	140	370	40	CC	486.4
test-13	20	4	160	370	60	SC	173.8
test-14	10	6	160	370	50	SC	125.6
test-15	40	8	160	370	40	CC	466.95
test-16	30	10	160	370	30	CC	495
test-17	40	4	100	520	30	CC	192.85
test-18	30	6	100	520	40	CC	211.35
test-19	20	8	100	520	50	CC	228.8
test-20	10	10	100	520	60	CC	143.1
test-21	40	4	120	520	40	CC	224.9
test-22	30	6	120	520	30	CC	203.15
test-23	20	8	120	520	60	CC	253.15
test-24	10	10	120	520	50	CC	171.95
test-25	30	4	140	520	50	SC	225.65
test-26	40	6	140	520	60	CC	317.2
test-27	10	8	140	520	30	CC	197.75
test-28	20	10	140	520	40	CC	281.22
test-29	30	4	160	520	60	SC	224.92
test-30	40	6	160	520	50	CC	347.44
test-31	10	8	160	520	40	SC	197.56
test-32	20	10	160	520	30	CC	304.5

* CC concrete cracking failure mode; SC shear connector failure mode

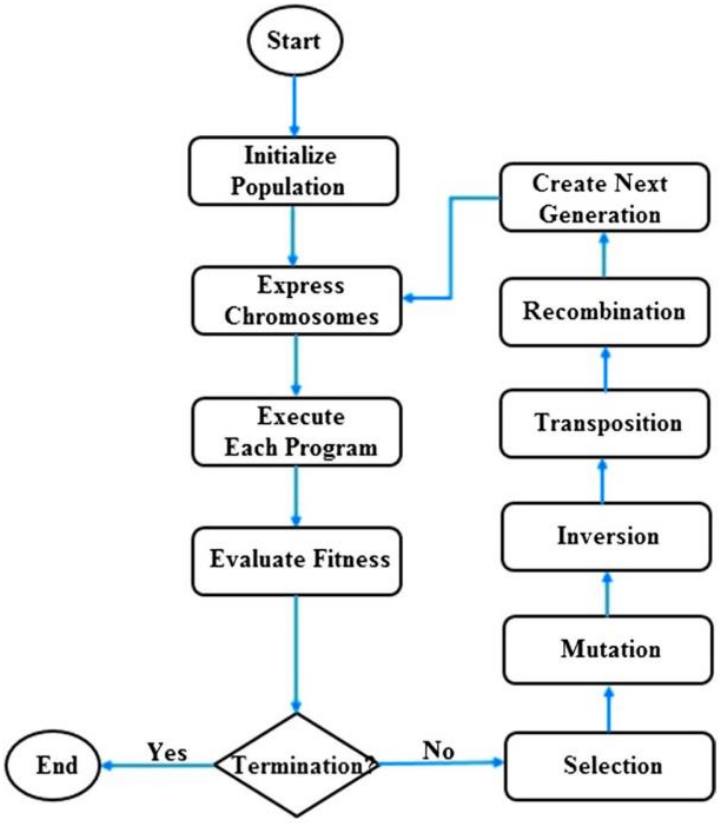

Fig. 10. GEP flowchart [32].

Table 6. GEP parameters.

Function set)	×Arctan, ÷,√ ,∛ ,
Head size	5
Chromosomes	50
Number of genes	2
Mutation rate	0.04
One-point recombination rate	0.3
Two-point recombination rate	03
Gene recombination rate	0.1
Gene transposition rate	0.1
Linking function	Multiplication

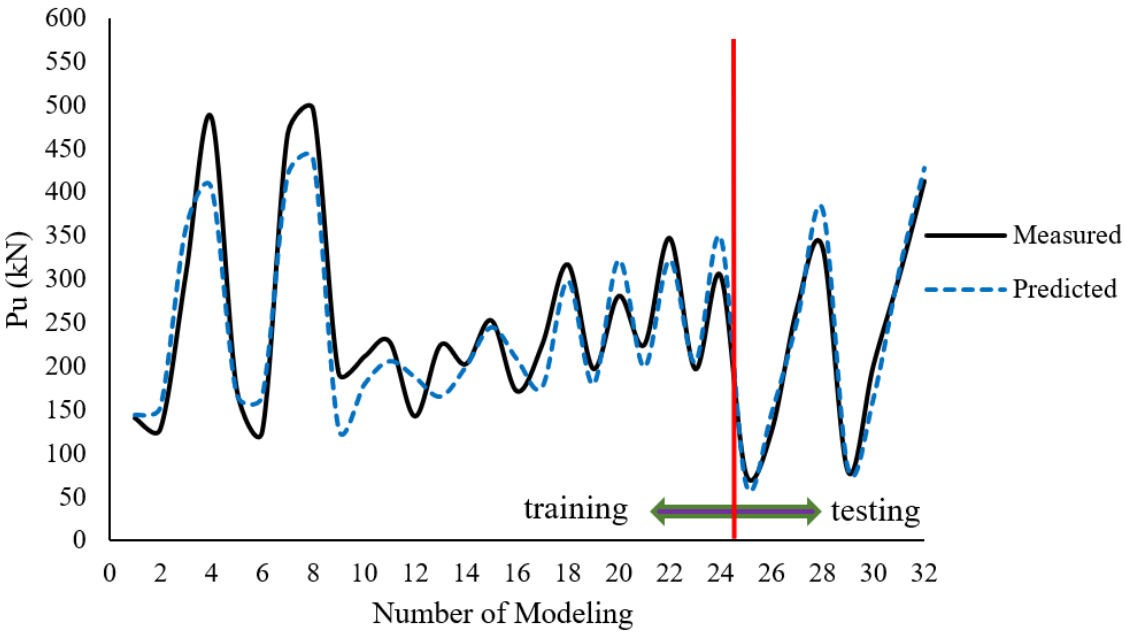

Fig. 11. GEP equation versus numerical data.

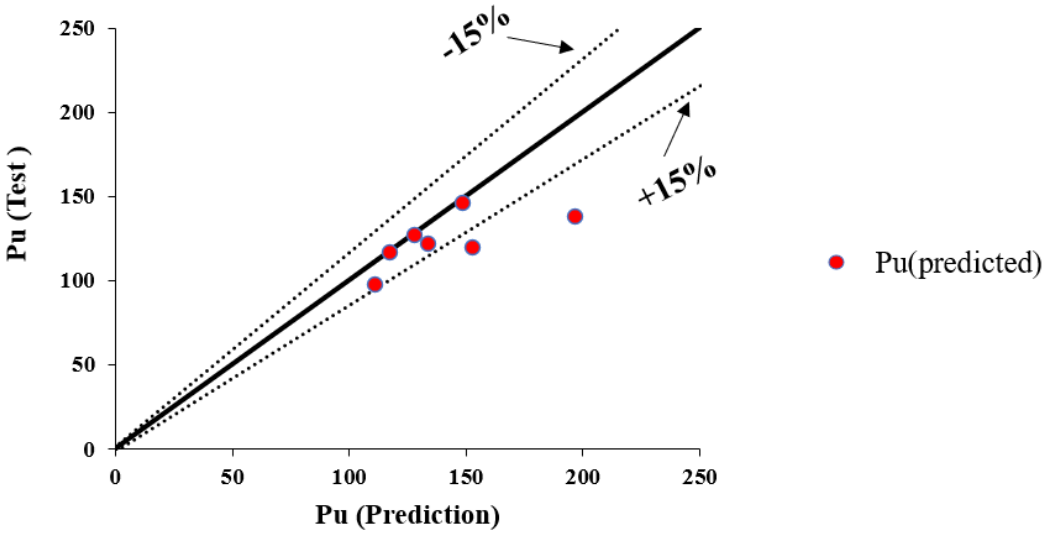

Fig. 12. GEP model vs. experimental results.

and BP height are the same. Fig. 11 compares the GEP equation to the numerical (training and testing) data.

8- Validation of the GEP model

The performance of the GEP model was evaluated by comparing its shear strength estimate to the experimental shear strength. Fig. 12 compares the experimental data and GEP estimates. A maximum error rate of 15% was regarded as the safe range. According to Fig. 12, most data points were in the safe range. Although the code provisions were developed for SCS sandwich structures with other shear connectors than BP connectors, the cost-effectiveness of BP connectors can be evaluated through a comparison of equations for a given steel faceplate cross-sectional area. Fig. 12 compares the proposed GEP equation to experimental results.

Table 7 provides the code provisions for the shear strength estimation of stud-bolt shear connectors. Since the stud-bolt shear connectors and BP shear connectors had different:

$$A_S = 2b_c t_c \tag{7}$$

Table 7. Comparison of the GEP model to code provisions.

Eurocode 4 (2004)[۳۳]	$P_u = \min\left(0.8 f_u \frac{\pi d^2}{4\gamma_v}, 0.29\alpha d^2 \frac{\sqrt{f_{ck}}}{\lambda_v}\right)$ $\alpha = 1, \gamma_v = 1.25$
ANSI/AISC 360-10[34]	$P_u = 0.5 A_s \sqrt{f_{cp} E_c} < 0.7 \gamma f_u A_s$
AASHTO Washington [35]	$P_u = 0.5 A_s \phi \sqrt{f_{ck} E_c} < \phi f_u A_s$
GB 50017 [29]	$P_u = 0.43 A_s \sqrt{f_{cp} E_c} < 0.7 \gamma f_u A_s$

*f_{ck} is the strength of cylindrical specimens, f_{cp} is the compressive strength of prismatic concrete, f_u id the ultimate tensile strength of stud-bolt shear connectors, E_c is the secant elasticity modulus of concrete, Ø is the factor of safety (0.85), and γ is the ratio of the minimum tensile strength to the yield point of stud-bolt shear connectors

Table 8. Comparison of the GEP model and code provisions to numerical and experimental results.

Spicemen	Pu_{exp} (kN)	prediction shear strength		Eurocode4		ANSI/AISC		AASHTO		GB50017	
		Pu (kN)	$\frac{Pu_{exp}}{Pu}$	Pu (kN)	$\frac{Pu_{exp}}{Pu}$	Pu (kN)	$\frac{Pu_{exp}}{Pu}$	Pu (kN)	$\frac{Pu_{exp}}{Pu}$	Pu (kN)	$\frac{Pu_{exp}}{Pu}$
N-1	111.41	97.05	1.15	40.16	2.78	46.8	2.38	53.04	2.10	43.68	2.55
N-2	153.25	118.86	1.29	60.14	2.55	70.2	2.18	79.56	1.93	65.52	2.34
N-3	196.92	137.25	1.43	80.19	2.46	93.6	2.10	106.08	1.86	87.36	2.25
N-4	134.24	121.31	1.10	50.12	2.68	80.25	1.67	90.95	1.48	74.9	1.79
N-5	148.93	145.57	1.02	60.14	2.48	91.8	1.62	104.04	1.43	85.68	1.74
N-6	118	116.46	1.01	40.1	2.94	49.8	2.37	56.44	2.09	46.64	2.53
N-7	128.5	126.16	1.02	40.1	3.20	52.2	2.46	59.16	2.17	48.72	2.64
AVE			1.057		2.72		2.11		2.082		2.52
C.O.V			0.028		0.0406		0.068		0.0595		0.0729

Table 8 compares the GEP model and code provisions in the shear strength estimation of seven experimental specimens. The mean and coefficient of variation (CV) were reported as 1.057 and 0.027 for the GEP model, respectively. Therefore, the GEP model outperformed the code provisions in the shear strength estimation of BP shear connectors.

The RMSE[1], MAPE[2], and NSE[3] were calculated to ensure the performance of the proposed GEP model[32]:

$$RMSE = \frac{\sqrt{\sum_{i=1}^{n}\left|\left(V_{\exp} - V_{pre}\right)^2\right|}}{n} \quad (8)$$

$$MAPE = \frac{\sqrt{\sum_{i=1}^{n}\left|\left(\frac{V_{\exp} - V_{pre}}{V_{\exp}}\right)\right|}}{n} \times 100 \quad (9)$$

1. Root-Mean-Square Error
2. Mean Absolute Percentage Error
3. Nash–Sutcliffe Efficiency

Table 9. Comparing error evaluation parameters.

Specimens by	parameter		
	RMSE	MAPE(%)	NSE
prediction by Eq(6)	2.65	2.97	0.987
Eurocode4	8.78	16.33	-10.37
ANSI/AISC	7.26	13.34	-6.76
AASHTO	6.37	11.67	-4.71
GB50017	7.71	14.18	-7.75

$$NSE = 1 - \frac{\sum_{i=1}^{n}\left(V_{\exp} - V_{pre}\right)^2}{\sum_{i=1}^{n}\left(V_{\exp} - \overline{V}_{\exp}\right)^2} \quad (10)$$

Where V_{exp}, V_{pri}, $\overline{V}_{exp}$, $\overline{V}_{pri}$, and n refer to the experimental shear strength, predicted shear strength, average experimental shear strength, average predicted shear strength, and the total number of specimens, respectively. The ideal RMSE, MAPE, and NSE would be 0, 0, and 1, respectively. Table 9 compares the equations based on the RMSE, MAPE, and NSE. The GEP model yielded an NSE of 0.987 and outperformed the other equations. It also had a MAPE of 1.766% and an RMSE of 0.938, showing the lowest errors. In conclusion, the proposed GEP equation had relatively good performance in the shear strength estimation of BP shear connectors.

9- Conclusion

This study evaluated BP shear connectors proposed by Khatibi *et al.* (2022) for SCS sandwich structures. Seven experimental push-out specimens were modeled and validated by comparing the experimental and numerical failure modes and load-slip curves. No equations had been introduced to estimate the shear strength of BP connectors, and code provisions developed for other shear connector shapes could not be reliable. Furthermore, the shear crack failure is an essential failure mode. Therefore, an equation with acceptable accuracy was developed using GEP to estimate the shear strength of SCS sandwich beams with BP shear connectors.

The Taguchi method was employed to design and simulate 32 specimens based on the mutual effects of BP thickness, width, and ultimate strength, and concrete core height and compressive strength. Then, an equation was developed using GEP to estimate the shear strength of BP connectors based on two failure modes: concrete core failure and steel faceplate failure.

$$p_u = \min\left\{\begin{array}{c} \sqrt{\sqrt{f_c}\times b_c}\times\dfrac{h_c\times t_c}{46.21} \\ \sqrt{\sqrt{f_u\times h_c}\times t_c\times b_c}\times\sqrt[3]{\mathrm{Arctan}\left(\dfrac{t_c}{f_u}\right)\times h_c} \end{array}\right\}$$

The GEP model was compared with experimental data and evaluated based on RMSE, MAPE, and NSE parameters. The NSE of the GEP model was reported as -0.39, suggesting that the GEP equation estimated higher BP shear strength than the code provisions. Therefore, the RMSE and MAPE were employed. The MAPE and RMSE of the GEP model were 2.97% and 2.65%, respectively, implying higher performance than the code provisions. In conclusion, the GEP model is expected to estimate the shear strength of BP connectors relatively well.

In future studies, computer vision algorithms can be utilized to automatically extract load-slip curves and detect failure modes in push-out tests. DeepLab and EfficientNet methods, leveraging image processing and deep learning, can enhance experimental data analysis and improve the validation of numerical models[36, 37].

Given the significance of investigating the behavior of BP connectors under cyclic and dynamic loading, it is recommended that future studies examine the effects of reduced ultimate strain in steel under these conditions. This can be achieved through cyclic testing and complementary numerical analyses to assess the accuracy of predictive equations for seismic scenarios.

References

[1] R.S.N. Shariati M, Shariati A, Kueh ABH, Comparative performance of channel and angle shear connectors in high-strength concrete composites: An experimental study, Constr Build Mater, (92) (2016) 120:382.

[2] N. Malek, Steel-concrete sandwich members without shear reinforcement, Transactions of Japan Concrete Institute (23) (1993) p 27–34.

[3] Z. Huang, J.R. Liew, Nonlinear finite element modelling and parametric study of curved steel–concrete–steel double skin composite panels infilled with ultra-lightweight cement composite, Construction and Building Materials, 95 (2015) 922–938.

[4] Y. Lin, J. Yan, Y. Wang, F. Fan, C. Zou, Shear failure mechanisms of SCS sandwich beams considering bond-slip between steel plates and concrete, Engineering Structures, 181 (2019) 458–475.

[5] Y. Lin, J. Yan, Z. Cao, X. Zeng, F. Fan, C. Zou, Ultimate strength behaviour of S-UHPC-S and SCS sandwich beams under shear loads, Journal of Constructional Steel Research, 149 (2018) 195–206.

[6] Z. Wang, J. Yan, Y. Lin, F. Fan, Y. Yang, Mechanical properties of steel-UHPC-steel slabs under concentrated loads considering composite action, Engineering Structures, 222 (2020) 111095.

[7] M. Xie, N. Foundoukos, J. Chapman, Experimental and numerical investigation on the shear behaviour of friction-welded bar–plate connections embedded in concrete, Journal of Constructional Steel Research, 61(5) (2005) 625–649.

[8] N. Anandavalli, J. Rajasankar, A. Prakash, B. Sivaprasad, Static response of steel-concrete-steel sandwich beam with bi-directionally inclined connectors, American Journal of Civil Engineering and Architecture, 1(1) (2013) 15–20.

[9] Y.-T. Guo, M.-X. Tao, X. Nie, S.-Y. Qiu, L. Tang, J.-S. Fan, Experimental and theoretical studies on the shear resistance of steel–concrete–steel composite structures with bidirectional steel webs, Journal of Structural Engineering, 144(10) (2018) 04018172.

[10] J.-B. Yan, Y.-Y. Yan, T. Wang, Z.-X. Li, Seismic behaviours of SCS sandwich shear walls using J-hook connectors, Thin-Walled Structures, 144 (2019) 106308.

[11] W. Zhang, Z. Huang, Z. Fu, X. Qian, Y. Zhou, L. Sui, Shear resistance behavior of partially composite Steel-Concrete-Steel sandwich beams considering bond-slip effect, Engineering Structures, 210 (2020) 110394.

[12] J.-B. Yan, H. Hu, T. Wang, Flexural behaviours of steel-UHPC-steel sandwich beams with J-hook connectors, Journal of Constructional Steel Research, 169 (2020) 106014.

[13] H. Roshani, M. Yousefi, N. Gharaei-Moghaddam, S.H. Khatibi, Flexural performance of steel-concrete-steel sandwich beams with lightweight fiber-reinforced concrete and corrugated-strip connectors: Experimental tests and numerical modeling, Case Studies in Construction Materials, 18 (2023) e02138.

[14] M. Yousefi, S.H. Khatibi, Experimental and numerical study of the flexural behavior of steel–concrete-steel sandwich beams with corrugated-strip shear connectors, Engineering Structures, 242 (2021) 112559.

[15] M. Yousefi, M. Ghalehnovi, Push-out test on the one end welded corrugated-strip connectors in steel-concrete-steel sandwich structure, Steel Compos. Struct, 24(1) (2017) 23–35.

[16] M. Yousefi, M. Ghalehnovi, Finite element model for interlayer behavior of double skin steel-concrete-steel sandwich structure with corrugated-strip shear connectors, Steel Compos. Struct, 27(1) (2018) 123–133.

[17] M. Daliri, H.G. Arab, M. Miri, S.H. Khatibi, Overlap effects of one-end welded box-profile shear connectors on interlayer shear behavior, in: Structures, Elsevier, 2025, pp. 107982.

[18] S.H. Khatibi, H.G. Arab, M. Miri, The behavior of steel-concrete-steel sandwich composite beams with box-profile shear connectors: Experimental and numerical, in: Structures, Elsevier, 2023, pp. 644–656.

[19] S.H. Khatibi, H.G. Arab, M. Miri, Interlayer behavior investigation of box profile shear connectors in steel-concrete-steel sandwich structures, in: Structures, Elsevier, 2022, pp. 1031–1042.

[20] K.M.A. Sohel, J.R. Liew, C.G. Koh, Numerical modelling of lightweight Steel-Concrete-Steel sandwich composite beams subjected to impact, Thin-Walled Structures, 94 (2015) 135–146.

[21] X.-L. Gao, J.-Y. Wang, C. Bian, R.-C. Xiao, B. Ma, Experimental investigation on the behaviour of UHPC-steel composite slabs under hogging moment, Steel and Composite Structures, An International Journal, 42(6) (2022) 765–777.

[22] J.-B. Yan, J.R. Liew, M.-H. Zhang, K. Sohel, Experimental and analytical study on ultimate strength behavior of steel–concrete–steel sandwich composite beam structures, Materials and Structures, 48 (2015) 1523–1544.

[23] Z. Huang, J.R. Liew, Structural behaviour of steel–concrete–steel sandwich composite wall subjected to compression and end moment, Thin-Walled Structures, 98 (2016) 592–606.

[24] C.-H. Li, J.-B. Yan, H.-N. Guan, Finite element analysis on enhanced C-channel connectors in SCS sandwich composite structures, in: Structures, Elsevier, 2021, pp. 818–837.

[25] M. Yousefi, M. Golmohammadi, S.H. Khatibi, M. Yaghoobi, Prediction of the punching load strength of SCS slabs with stud-bolt shear connectors using numerical modeling and GEP algorithm, Journal of Rehabilitation in Civil Engineering, 11(3) (2023) 68–87.

[26] J.-b. Yan, J.R. Liew, K. Sohel, M. Zhang, Push-out tests on J-hook connectors in steel–concrete–steel sandwich structure, Materials and structures, 47 (2014) 1693–1714.

[27] A. Karimipour, M. Ghalehnovi, M. Golmohammadi, J. De Brito, Experimental investigation on the shear behaviour of stud-bolt connectors of steel-concrete-steel fibre-reinforced recycled aggregates sandwich panels, Materials, 14(18) (2021) 5185.

[28] A.S.U.s. Manual, Abaqus 6.11, http://130.149, 89(2080) (2012) v6.

[29] A. Kumar, S. Clement, V. Agrawal, Optimum selection and ranking of electroplating system process parameters: Taguchi-MADM approach, International Journal of Applied Decision Sciences, 4(4) (2011) 341–361.

[30] D. Muñoz, Thesis Discovering unknown equations that describe large data sets using genetic programming techniques, Master›s Thesis, Linköping Institute of Technology, 2005.

[31] P. Sarir, J. Chen, P.G. Asteris, D.J. Armaghani, M. Tahir, Developing GEP tree-based, neuro-swarm, and whale optimization models for evaluation of bearing capacity of concrete-filled steel tube columns, Engineering with Computers, 37 (2021) 1–19.

[32] D. Jahed Armaghani, R.S. Faradonbeh, E. Momeni, A. Fahimifar, M. Tahir, Performance prediction of tunnel boring machine through developing a gene expression programming equation, Engineering with Computers, 34 (2018) 129–141.

[33] P. Code, Eurocode 2: design of concrete structures-part 1–1: general rules and rules for buildings, British Standard Institution, London, 668 (2005) 659–668.

[34] A. Specification, Specification for structural steel buildings, ANSI/AISC, 36010 (2005).

[35] L. Aashto, Bridge design specifications, (1998).

[36] H. Kabir, J. Wu, S. Dahal, T. Joo, N. Garg, Automated estimation of cementitious sorptivity via computer vision, Nature Communications, 15(1) (2024) 9935.

[37] Z. Song, S. Zou, W. Zhou, Y. Huang, L. Shao, J. Yuan, X. Gou, W. Jin, Z. Wang, X. Chen, Clinically applicable histopathological diagnosis system for gastric cancer detection using deep learning, Nature Communications, 11(1) (2020) 4294.

HOW TO CITE THIS ARTICLE

S. H. Khatibi, H. Ghohani Arab, M. Miri, Prediction of the shear strength of SCS Panel with Box Profile shear connectors using numerical modeling and GEP algorithm, AUT J. Civil Eng., 9(2) (2025) 111-128.

DOI: 10.22060/ajce.2025.23851.5904